Materials Chemistry and Physics 171 (2016) 178–184

Contents lists available at ScienceDirect

Materials Chemistry and Physics

journal homepage: www.elsevier.com/locate/matchemphys

Microstructure, interparticle interactions and magnetotransport of manganite-polyaniline nanocomposites

Mariano Romero [a, b], Ricardo Faccio [a, b], Helena Pardo [a, b], Milton A. Tumelero [c], Cristiani Campos Plá Cid [d], André A. Pasa [c, d], Álvaro W. Mombrú [a, b, *]

[a] Centro NanoMat/Cryssmat Lab, DETEMA, Facultad de Química, Universidad de la República, Uruguay
[b] Centro Interdisciplinario de Nanotecnología, Química y Física de Materiales, Espacio Interdisciplinario, Universidad de la República, Uruguay
[c] Laboratorio de filmes finos e superficies, Departamento de Física, Universidad Federal de Santa Catarina, Florianópolis, Brazil
[d] Laboratorio Central de Microscopia Electronica, Universidad Federal de Santa Catarina, Florianópolis, Brazil

HIGHLIGHTS

- A SAXS study on the microstructure of manganite-polyaniline nanocomposites is reported.
- We report the presence of attractive interactions for the composites with higher concentration in manganite.
- Interparticle dipole–dipole interactions were estimated by means of the SAXS interference function.
- Coercive field and remanent magnetization studies showed agreement with SAXS analysis.
- Magnetotransport showed an enhancement in relation to the decrease of these interactions.

GRAPHICAL ABSTRACT

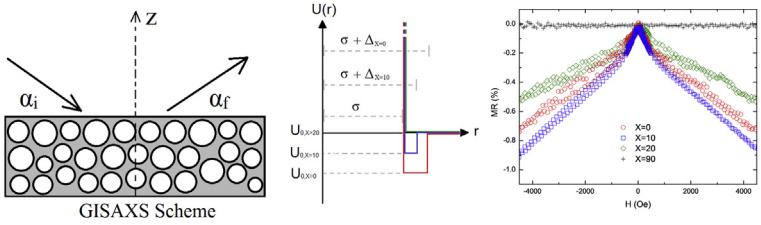

ARTICLE INFO

Article history:
Received 15 October 2015
Received in revised form
15 December 2015
Accepted 3 January 2016
Available online 11 January 2016

Keywords:
Composite materials
Magnetic materials
Microstructure
Transport properties

ABSTRACT

In this report, we present the study on the microstructure and interparticle interactions of manganite-polyaniline nanocomposites using grazing incidence small angle X-ray scattering (SAXS). In order to determine the nanoparticles mean diameter and correlation distances, data analysis was performed using the Guinier and Beaucage fits, in good agreement with transmission electron microscopy and X-ray diffraction analysis. The analysis of the interference functions revealed the existence of attractive interactions between nanoparticles. The nanocomposites with higher manganite concentration showed best fitting using the sticky hard sphere approximation. A weakening in the attractive interaction with increasing the dilution of nanoparticles in the polymer matrix was observed until a critical volume fraction ($\phi_c \sim 0.4$) is reached, upon which the hard sphere approximation showed best fitting. The interaction potentials were estimated at room temperature revealing a decrease in the depth and width of the square well with increasing nanoparticle dilution. Coercive field and remanent magnetization showed a decrease with increasing polymer addition suggesting the declining of dipole–dipole interactions, in agreement with SAXS analysis. Magnetoresistance also showed an enhancement that could

* Corresponding author. Centro NanoMat/Cryssmat Lab, DETEMA, Facultad de Química, Universidad de la República, Uruguay.
E-mail address: amombru@fq.edu.uy (Á.W. Mombrú).

http://dx.doi.org/10.1016/j.matchemphys.2016.01.003

be probably associated to the decrease in the dipole–dipole interactions between ferromagnetic $La_{2/3}Sr_{1/3}MnO_3$ (LSMO) nanoparticles at a critical separation distance in these nanocomposites.

1. Introduction

There is a recent interest in the magnetotransport properties of spin valves based in nanocomposite materials in relation with colossal magnetoresistance [1] and magnetic tunneling junction devices [2]. The magnetoresistance (MR) phenomenon is explained on the basis of the spin polarized tunneling between magnetic phases through a few nanometer width insulator layers. The enhancement of the MR, due to the alignment of neighboring ferromagnetic grains is promoted by the grain boundaries, which act as pinning centers for the demagnetization. Moreover, the grain boundary disorder is also crucial to produce a higher spin disorientation of the magnetic virgin state in order to achieve an enhancement in the magnetoresistance at low applied magnetic fields [3,4].

With this in mind, many studies have focused in the preparation of nanocomposite materials in order to control the microstructure and thus adjusting the tunneling barrier to achieve an enhancement in the low field magnetoresistance (LFMR). The most common materials used for this purpose are composites with the ferromagnetic $La_{2/3}Sr_{1/3}MnO_3$ (LSMO) manganite nanoparticles embedded in a polymer matrix such as polymethylmetacrilate (PMMA) [3,4], polyparaphenylene (PPP) [5], paraphenylsulfide (PPS) [6], polyethyleneglycol (PEG) [7] and more recently, the conductive polymer polyaniline (PANI) [8]. In previous reports, we focused in the compositional and structural characterization on the interphase of these nanocomposites and its influence on the magnetotransport properties [9,10]. Nevertheless, there are still very few reports regarding the study of the microstructure and interparticle interactions based in small angle X-ray scattering (SAXS) technique for these types of materials. In this report, we present a detailed study on the microstructure and interparticle interactions of manganite-polyaniline nanocomposites using grazing incidence small angle X-ray scattering (GISAXS). As far as we know, we present, for the first time, an estimation based in experimental SAXS data on the interaction potentials energies involved in these manganite-polymer nanocomposite materials interphase. Additionally, we show the existence of a correlation between dipole–dipole interactions with magnetotransport across the tunnel barrier in the interphase of these nanocomposite materials.

2. Materials and methods

LSMO nanoparticles were prepared using the polymer precursor method as described in previous reports [9,10]. LSMO nanoparticles and PANI emeraldine salt powder were mixed, grinded and pelletized at a pressure of 50 kN during 10 min. The pellets were annealed at T = 200 °C during 30 min under a 20 mL/min nitrogen flow.

TEM images were taken at 100 kV using a JEOL JEM 1010 and HR-TEM images were taken at 200 kV using a JEOL JEM 2100, after previous dispersion of the powders in isopropyl alcohol, sonication in aqueous bath for 10 min and deposition onto a carbon holey film. Grazing incidence X-ray diffraction (GIXRD) was performed using a Rigaku Ultima IV with CuKα radiation operated at 40 kV and 30 mA, in the 2θ range = 5–75°, with a 5 seconds step of 0.02°. Grazing incidence small angle X-ray scattering experiments were carried out using parallel beam collimated CuKα radiation directly onto the LSMO-PANI-X compressed pellets surface. Previous reflectometry analysis was performed to determine the critical angle (α_c) and fix the working angle at $\alpha_i \sim 0.3°$, in order to have a radiation depth in the order of a few nanometers and the scattering radiation was collected for the out-of-plane direction in the scattering vector range q = 0.003–0.12 $Å^{-1}$. I(q) vs q curve analysis was performed using the Beaucage method [11,12] and S(q) vs q analysis was performed using the perturbative solution of the Percus-Yevick closure, according to the sticky hard sphere approximation proposed by Baxter [13] using SASview 3.0 software. Magnetization measurements were performed at room temperature in a VSM-Microsense EV9 vibrating sample magnetometer. Resistivity (ρ) measurements were obtained at room temperature by the four-probe technique and magnetoresistance (MR) was calculated following $MR(\%) = 100(\rho_H - \rho_0)/\rho_0$, with ρ_H as the resistivity with ($0 < H < 4.5$ kOe) and ρ_0 as the resistivity without applied magnetic field (H = 0).

3. Results and discussion

3.1. Transmission electron microscopy

TEM images for LSMO-PANI-X nanocomposites after grinding and re-suspension are shown in Fig. 1. In all images, the presence of clusters of nanoparticles is observed. X = 0 clustering could be ascribed to the partial sintering and X = 10 and 20 is mostly due to the polymer mediated binding. LSMO nanoparticles microstructure can be described as polyhedra with a rounded-shape sized between D_m = 30–50 nm. HR-TEM images (Fig. 1) showed different local separation distances (d) between nanoparticles for the different amounts of polymer additions, with d ~ 0, 1.5 and 2.0 nm for X = 0, 10 and 20, respectively.

3.2. Grazing incidence X-ray diffraction

GIXRD patterns are shown in Fig. 2 for LSMO-PANI-X with X = 0, 10, 20, 90 and 100. X = 100 confirmed the presence of polyaniline in its emeraldine salt form, denoted by the presence of broad peaks at 2θ = 15.4, 19.8 and 25.2°, assigned to (001), (100) and (110) *h k l* reflections with associated d_{hkl} = 6.0, 4.4 and 3.5 Å, respectively [14,15]. X = 0, 10, 20 and 90 showed the presence of LSMO perovskite with an orthorhombic structure in the *Pbnm* spacegroup as it was reported previously [9,10] and its corresponding *hkl* reflections are marked in Fig. 2. The mean crystallite diameter applying the Scherrer equation (D_s) showed a slight decrease from D_s = 23 to 20 nm with increasing X, as it is shown in Table 1. This slight decrease in the crystallite size could be ascribed to the formation of local amorphous regions at the LSMO grain boundaries promoted by the addition of the polymer. However a lower accuracy in the mean crystallite size estimation due to diluting effects into the amorphous polyaniline should also be considered.

3.3. Grazing incidence small angle X-ray scattering

In order to analyze GISAXS data, the surface roughness